Slow light using spectral hole burning in a Tm^{3+}-doped yttrium-aluminum-garnet crystal

R. Lauro,* T. Chanelière, and J. L. Le Gouët
Laboratoire Aimé Cotton, Université Paris-Sud, CNRS-UPR 3321, Bât. 505, 91405 Orsay Cedex, France
(Received 29 January 2009; published 30 June 2009)

We report on light slowing down in a rare-earth-metal-ion-doped crystal by persistent spectral hole burning. The absence of motion of the active ions, the large inhomogeneous broadening, the small homogeneous width, and the long lifetime of the hyperfine shelving states make this material convenient for the burning of narrow persistent spectral holes. Since the hole can be burnt long before the arrival of the input signal, there is no need for a strong-coupling field, illuminating the sample simultaneously with the input signal, in contrast with procedures such as electromagnetically induced transparency or coherent population oscillations. Analyzing the slowing down process, we point out the role played by the off-resonant atom. Most of the incoming information is carried over to off-resonant atoms, while the pulse is confined within the sample. The observed speed-of-light reduction factor exceeds 10^5.

DOI: 10.1103/PhysRevA.79.063844 PACS number(s): 42.25.Bs, 42.50.Gy, 42.50.Ct, 42.50.Md

I. INTRODUCTION

A light pulse can propagate in a resonant medium faster or slower than in vacuum. This is a consequence of the wave nature of light [1]. In addition to arousing an everlasting basic interest [2–4], the speed-of-light control may have practical applications in nonlinear optics [5] and optical information processing [6]. Moreover, slow light has been brought into play in quantum storage investigations where a quantum state of light is mapped into an atomic ensemble [7].

Most of slow light experiments are based on electromagnetically induced transparency (EIT) [8] in cold atoms [9], warm vapors [10], as well as in rare-earth-metal-ion-doped solids [11,12] and nitrogen vacancy centers in diamond [13]. Coherent population oscillations (CPOs) [14] also lead to large group delays [15,16]. However, in both EIT and CPO protocols, a strong-coupling field has to be shined to the atoms simultaneously with the signal pulse. The intense coupling field may hamper the monitoring and detection of the weak probe.

Recently, it has been proposed to use spectral hole burning (SHB) for reducing the speed of light [17,18]. So far, this was demonstrated in hot rubidium vapor [19]. In the present paper we investigate SHB slowing down in rare-earth ion-doped crystals (REIC). Indeed, such materials exhibit some attractive features. Since the active ions do not move, the hole lifetime is not limited by atomic diffusion. In addition, one can take advantage of the slow hyperfine relaxation to burn long lifetime holes by shelving the burnt atoms in a ground-state hyperfine level. Hence, one can send the signal pulse after the hole has been burnt, unlike in vapor experiments [19], where pump and signal fields must overlap in time. Moreover, with an optical dipole lifetime of tens of microseconds, typically 4 orders of magnitude larger than in alkaline atoms, one can burn holes as narrow as a few hundreds of kHz, which may lead to a dramatic reduction of the group velocity. Finally, the large ratio between inhomogeneous and homogeneous broadenings available in REIC offers possibilities for multimode delay lines.

The paper is comprised of a theoretical discussion and an experimental report. The theoretical discussion leads us to emphasize the role played by the off-resonant centers that adiabatically follow the propagating light pulse. As shown in a parent paper [20], this slowing down mechanism can be extended into a quantum storage protocol where the optical information is carried over to a ground-state coherence in the off-resonant atoms. The experimental report is devoted to the slow light results obtained in a Tm^{3+}-doped yttrium-aluminum-garnet (YAG) crystal.

II. SLOW LIGHT PROPAGATION IN A SPECTRAL HOLE: ATOMIC RESPONSE AND ENERGY TRANSFER

An electromagnetic signal of frequency ω_0 propagating in a dispersive medium has a group velocity $c/[n+\omega_0(dn/d\omega)]$, where $n(\omega)$ is the refractive index. Provided the quantity, $dn/d\omega$, is larger than $1/\omega_0$, the speed of light is reduced. As shown by Kramers Kronig relations, the refractive index may exhibit such a strong positive slope when a transparency window (TW) is opened in an absorbing medium. The group velocity v_g is of the order Δ_0/α_0, where Δ_0 and α_0, respectively, stand for the TW width and the absorption coefficient outside TW. The deeper and the narrower the TW, the smaller is the group velocity. Such a TW is the basic ingredient of hole burning spectroscopy in inhomogeneously broadened materials. The burning laser modifies the atomic population distribution over a spectral interval that is larger than the homogeneous width, but narrower than the inhomogeneous one. If SHB slowing down is performed in an ensemble of two-level atoms [17,18], the linear absorption coefficient depends on the atomic level population difference and transparency is obtained if both ground and excited populations are equal. Then, the spectral hole lifetime is limited by the excited-state lifetime. In three-level Λ-like atoms, optical pumping to a shelving state may lead to a much longer hole lifetime. In REIC, such Λ systems can be built on the ground-state hyperfine structure, with a corresponding lifetime of up to a few days [21].

*romain.lauro@lac.u-psud.fr

An incoming signal pulse, narrower than the previously burnt spectral hole, shall exit the medium with little shape distortion and energy loss. However, during its propagation through the sample at velocity v_g, the signal is spatially compressed by a factor v_g/c. If the medium is thick enough to accommodate the entire compressed pulse, the optically carried energy is reduced by the same factor. Hence, if $v_g \ll c$, the pulse abandons most of its energy during its propagation through the medium, but recovers this energy at the exit. This energy must be temporarily stored somehow in the material.

The relationship between slowing down and energy transfer to the active atoms was explained in terms of adiabatic following by Grischkowsky [22] in the case of an optical pulse tuned to a wing of an absorption line in rubidium vapor. In Ref. [22], since the optical detuning is much larger than the inhomogeneous linewidth, atoms are all excited in the same way. We extend Grischkowsky's work to spectral hole burning conditions, where the off-resonant atoms are spread over the inhomogeneous linewidth.

We consider an ensemble of two level atoms. The transition at frequency ω_{12} between the ground and upper states $|1\rangle$ and $|2\rangle$ is excited by a weak signal field $E(z,t) = \frac{1}{2}\mathcal{E}(z,t)e^{i(kz-\omega_l t)} + \text{c.c.}$, where $k=\omega_l/c$. Within the framework of the rotating wave approximation, the optical Bloch equations read as

$$\dot{\tilde{\sigma}}_{21}(z,t) = \frac{i}{2}\Omega(z,t)w(z,t) - \left(i\Delta + \frac{1}{T_2}\right)\tilde{\sigma}_{21}(z,t), \tag{1}$$

$$\dot{w}(z,t) = -i\Omega(z,t)[\tilde{\sigma}_{12}(z,t) - \tilde{\sigma}_{21}(z,t)] + \frac{1}{T_1}[1 - w(z,t)], \tag{2}$$

where $\sigma_{ij}(z,t) = \tilde{\sigma}_{ij}(z,t)e^{i(kz-\omega_l t)}$ stands for the optical coherence, $w(z,t) = \sigma_{11} - \sigma_{22}$ represents the level population difference, $\Omega(z,t) = \mu_{12}\mathcal{E}(z,t)/\hbar$ is the Rabi frequency (μ_{12} is the dipole moment matrix element), T_1 and T_2 are the longitudinal and transverse relaxation times, respectively, and $\Delta = \omega_{12} - \omega_l$ is the optical detuning. Since the probe pulse is weak, $w(z,t) \approx 1$ and the optical coherence reduces to

$$\tilde{\sigma}_{21}(z,t) = \frac{i}{2}e^{-(i\Delta+1/T_2)t}\int_{-\infty}^{t}\Omega(z,t')e^{(i\Delta+1/T_2)t'}dt'. \tag{3}$$

With the condition $\lim_{t\to-\infty}\Omega(t)=0$, repeated integration by parts leads to

$$\tilde{\sigma}_{21}(z,t) = -\frac{i}{2}\sum_{n=0}^{\infty}\left(\frac{-1}{i\Delta + 1/T_2}\right)^{n+1}\frac{\partial^n}{\partial t^n}\Omega(z,t). \tag{4}$$

In terms of the atomic coherence, the macroscopic density of polarization reads as $P(z,t) = \mu_{12}\int G(\omega_{12})[\sigma_{12}(z,t) + \sigma_{21}(z,t)]\,d\omega_{12}$, where $G(\omega_{12})$ represents the atomic inhomogeneous distribution of width Γ_{inh}.

Spectral hole burning modifies the inhomogeneous distribution (Fig. 1). We assume that both $G(\omega_{12})$ and the spectral hole are centered at ω_l. Let the hole be given a Lorentzian shape of width $\Delta_0 \ll \Gamma_{inh}$. Then the modified inhomogeneous distribution reads as $G'(\omega_{12}) = G(\omega_{12})\{1 - (\Delta_0^2/4)/[(\omega_{12} - \omega_l)^2 + \Delta_0^2/4]\}$. Hence, the positive frequency component of polarization can be written as

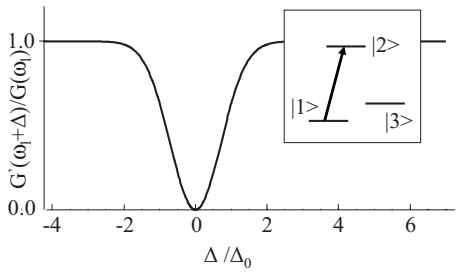

FIG. 1. Inhomogeneous distribution $G'(\Delta+\omega_l)/G(\omega_l)$ with a Δ_0-wide spectral hole. Inset represents the Λ-shape three-level system. The input signal pulse excites the transition 1–2.

$$\mathcal{P}(z,t) = -i\frac{\mu_{12}}{2}\sum_{n=0}^{\infty}\frac{\partial^n}{\partial t^n}\Omega(z,t)\int_{-\infty}^{\infty}G(\Delta+\omega_l)\left(\frac{-1}{i\Delta + 1/T_2}\right)^{n+1} \times\left(1 - \frac{\Delta_0^2/4}{\Delta^2 + \Delta_0^2/4}\right)d\Delta. \tag{5}$$

The hole must be broader than the pulse spectrum and the pulse duration must be shorter than the dephasing time T_2, which entails the condition $1/T_2 \ll \Delta_0 \ll \Gamma_{inh}$.

Only atoms outside the hole, i.e., with $\Delta > \Delta_0$, contribute to the integral in Eq. (5). For these atoms, one can write $(-1/[i\Delta + 1/T_2])^{n+1} \approx (i/\Delta)^{n+1}$. For parity reasons, only odd n index contributes. Moreover, considering that the signal pulse varies slowly on $1/\Delta_0$ time scale, Eq. (5) can be reduced to the $n=1$ leading term. Keeping in mind that inhomogeneous broadening is much larger than $1/T_2$ and Δ_0, one can write the macroscopic polarization as

$$\mathcal{P}(z,t) = \frac{i\mu_{12}^2 G(\omega_l)}{2\hbar}\frac{\partial}{\partial t}\mathcal{E}(z,t)\int_{-\infty}^{\infty}\left(\frac{1}{\Delta^2}\right)\left(1 - \frac{\Delta_0^2/4}{\Delta^2 + \Delta_0^2/4}\right)d\Delta = i\frac{\pi\mu_{12}^2 G(\omega_l)}{\hbar\Delta_0}\frac{\partial}{\partial t}\mathcal{E}(z,t). \tag{6}$$

Inserting $\mathcal{P}(z,t)$ into the linearized propagation equation

$$\frac{\partial}{\partial z}\mathcal{E}(z,t) + \frac{1}{c}\frac{\partial}{\partial t}\mathcal{E}(z,t) = i\frac{k}{\epsilon_0}\mathcal{P}(z,t) \tag{7}$$

leads to the traveling-wave equation

$$\frac{\partial}{\partial z}\mathcal{E}(z,t) + \left(\frac{1}{c} + \frac{\alpha_0}{\Delta_0}\right)\frac{\partial}{\partial t}\mathcal{E}(z,t) = 0, \tag{8}$$

where we have substituted the linear absorption coefficient $\alpha_0 = \pi k G(\omega_l)\mu_{12}^2/\hbar\epsilon_0$. The signal propagates without distortion at velocity v_g given by

$$1/v_g = 1/c + \alpha_0/\Delta_0. \tag{9}$$

In REIC, typical values of α_0 and $\Delta_0/2\pi$ are around 10^3 m^{-1} and 100 kHz, respectively, which leads to a light velocity reduction factor $v_g/c \approx 3\times10^{-6}$. At the input and

output sides of the medium the signal pulse amplitude is preserved since the index of refraction is unity. Hence, the signal pulse inside medium reads as

$$\mathcal{E}^{in}(z,t) = \mathcal{E}^{out}(z=0, t - z/v_g), \tag{10}$$

where $\mathcal{E}^{in}(z,t)$ and $\mathcal{E}^{out}(z,t)$, respectively, stand for the electric fields inside and outside medium.

We turn now to the energy transfer from light to atoms. From Eq. (2), we can express the excited population as

$$\sigma_{22}(z,t) = \frac{i}{2} e^{-t/T_1} \int_{-\infty}^{t} \Omega(z,t')[\tilde{\sigma}_{12}(z,t) - \tilde{\sigma}_{21}(z,t)] e^{t'/T_1} dt'. \tag{11}$$

Since both the pulse duration and the propagation time are $\ll T_1$, Eq. (11) can be written as

$$\sigma_{22}(z,t) = \int_{-\infty}^{t} \Omega(z,t') \mathrm{Im}[\tilde{\sigma}_{21}(z,t')] dt'. \tag{12}$$

For off-resonant atoms such that $\Delta \gg 1/T_2, \Delta_0$, the coherence reduces to the leading $n=1$ term of Eq. (4). Therefore $\mathrm{Im}(\sigma_{21}) = \frac{\partial}{\partial t}\Omega/(2\Delta^2)$. Substituting this expression in Eq. (11), one obtains

$$\sigma_{22}(z,t) = \frac{1}{2\Delta^2} \int_{-\infty}^{t} \Omega(z,t') \frac{\partial}{\partial t'} \Omega(z,t') dt' = \frac{1}{4} \left(\frac{\Omega(z,t)}{\Delta} \right)^2. \tag{13}$$

Integration over the spatial and spectral atomic distributions finally leads to the energy stored in the atoms at time t,

$$\begin{aligned} W_{at} &= \frac{\mu_{12}^2 \omega_{12}}{4\hbar} \int_0^L |\mathcal{E}^{in}(z,t)|^2 dz \int_{-\infty}^{\infty} \frac{1}{\Delta^2} G(\Delta + \omega_l) \\ &\quad \times \left(1 - \frac{\Delta_0^2/4}{\Delta^2 + \Delta_0^2/4} \right) d\Delta \\ &= c \frac{\alpha_0}{\Delta_0} \frac{\epsilon_0}{2} \int_0^L |\mathcal{E}^{in}(z,t)|^2 dz. \end{aligned} \tag{14}$$

In terms of the optically carried energy inside the medium, $W_{em}^{in} = \epsilon_0/2 \int_0^L |\mathcal{E}^{in}(z,t)|^2 dz$, and of the group velocity [see Eq. (9)], Eq. (14) can be expressed as

$$W_{at} = \left(\frac{c}{v_g} - 1 \right) W_{em}^{in}. \tag{15}$$

Therefore, in the slow light regime, most of the energy is stored in the atoms.

In the above discussion both the slowing down process and the temporary energy transfer to off-resonance atoms are derived from the Maxwell-Bloch equations. At the end we verify the energy conservation. A different approach may be considered, where the speed of light reduction is derived from the conservation of energy. As the signal wave travels through the medium, the off-resonance atoms stay in the adiabatic state $c_+(z,t)|1\rangle + c_-(z,t)|2\rangle$, where $c_\pm(z,t) = [\sqrt{\Omega(z,t)^2 + \Delta^2} \pm \Delta]^{1/2} / \sqrt{2}[\Omega(z,t)^2 + \Delta^2]^{1/4}$. Expanding state $|2\rangle$ population in powers of Ω/Δ, one recovers Eq. (13). Summing the excited-state energy over all the atoms leads to Eq. (14). The conservation of energy can be expressed as $W_{em}^{out} = W_{at} + W_{em}^{in}$. The energy carried by the signal pulse before entering the medium, W_{em}^{out}, is shared between the atoms and the electromagnetic field when the pulse is confined in the medium. Besides, $W_{em}^{in} = W_{em}^{out} v/c$, since the light pulse behaves as a traveling wave. Hence the group velocity inside the medium is finally given by $v/c = (W_{em}^{out} - W_{at})/W_{em}^{out}$.

Rather paradoxically, the total energy travels at group velocity in the medium, as confirmed by the light pulse revival at the exit of the sample, although the electromagnetic field carries nearly no energy inside the medium. This is rather surprising since the energy can only be transported by this weak field. The consistency can only be restored if the optically carried energy travels at speed c. Indeed, let U_{em}^{in} (respectively U_{at}) be the energy density carried by the electromagnetic field (respectively, stored in the atoms). The total flux of energy through a section perpendicular to propagation direction is $(U_{em}^{in} + U_{at}) v_g$. This coincides with the flux of electromagnetic energy, provided the latter quantity is given by $U_{em} c$, as can be easily derived from Eq. (15). This problem was already addressed in Ref. [23], in the framework of self-induced transparency [24].

III. EXPERIMENTS

We investigate slow light propagation through a spectral hole in a thulium-doped YAG crystal. This material fulfills two essential conditions for spectral hole burning. First, the inhomogeneous broadening ($\Gamma_{inh} \approx 20$ GHz) is much larger than the homogeneous linewidth ($\gamma_{hom} \approx 10$ kHz at 1.8K). Second, thulium ions exhibit a double lambda structure in the presence of a properly oriented external magnetic field. This four-level structure consists of two ground and two excited hyperfine sublevels [25]: one of the ground states can be used as a shelving state for persistent spectral hole burning.

The setup is represented in Fig. 2. The system is shined by an extended cavity diode laser (ECDL) operating at 793 nm, stabilized on a high finesse Fabry-Pérot cavity through a Pound-Drever-Hall servoloop. The laser linewidth is reduced to 200 Hz over 10 ms [26]. A semiconductor tapered amplifier (Toptica BoosTA) is used to raise the beam intensity.

We resort to acousto-optic modulators (AOMs) for the temporal shaping of the optical-field phase and amplitude. Spatial filtering by a single mode fiber precisely controls the spatial phase and amplitude. However, combining temporal and spatial controls requires some care. Indeed, the direction of an AOM deflected beam varies with the driving rf. In double-pass configuration, the beam emerges in fixed direction but a single AOM is then not enough to carry over an arbitrary phase and amplitude shaping onto the optical field. For instance, modulation at rf frequencies f_1 and f_2 in double-pass arrangement gives rise to shifted components not only at $2f_1$ and $2f_2$, but also at $f_1 + f_2$. To get rid of this beat note, one has to use two distinct AOMs, each one being driven at a single rf frequency. On that purpose the laser beam is directed to a polarizing beam splitter that separates the two orthogonal light polarizations. Each one of the split

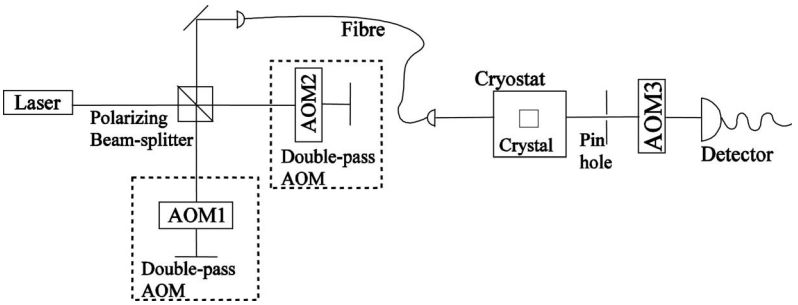

FIG. 2. Experimental setup. The acousto-optic modulators AOM1 and AOM2 are set in double-pass configuration so that the deflected beam direction does not vary with the rf driving frequency. Various beams are all put into the unique spatial mode of a single-mode fiber before reaching the liquid-helium-cooled crystal. AOM3 is used as a gate to protect the detector from the intense preparation pulses.

beams is double passed through an AA Opto-Electronic acousto-optic modulator centered at 110 MHz. The two AOMs are independently and synchronously driven by a dual-channel 1 gigasample/s waveform generator (Tektronix AWG520) that can provide arbitrary amplitude and phase shaping. Each channel feeds one frequency shift at a time. After passing twice through the AOMs, the split beams come back to the cube where they merge. The recombined beam is routed in a fixed direction, insensitive to frequency shift. The merged beam is finally coupled into a monomode fiber. Therefore all the optical-field components propagate along the same spatial mode whatever their frequency. The beam is then focused on a 0.5 at. % Tm^{3+}:YAG sample cooled down to 1.7 K in an Oxford Spectromag cryostat. The magnetic field generated by superconducting coils is applied in the direction giving maximum branching ratio [25]. The spot diameter on the crystal is adjusted to 80 μm. Sample is then imaged onto a 50-μm diameter pinhole with a magnification factor of 2. The transmitted light is collected on an avalanche photodiode HAMAMATSU C5460 or C4777 protected from strong excitation pulses by a third AOM used as a variable density filter.

Persistent spectral hole burning in Tm:YAG is described in Ref. [27] and is illustrated on Fig. 3. At 1.8 K, both ground states are equally populated. The crystal is illuminated by a laser at frequency ν_0. Due to inhomogeneous broadening, the laser simultaneously excites four classes of ions and optical pumping tends to unbalance the ground level distribution around excitation frequency ν_0. A weak probe pulse absorption depends on the ground-state population. Hence, around ν_0 and $\nu_0 \pm \Delta_e$, a hole is burnt in the absorption profile. Conversely, around $\nu_0 \pm \Delta_g$ and $\nu_0 \pm (\Delta_g - \Delta_e)$, an antihole reflects an absorption increase. In Fig. 3(b) we show an absorption spectrum, when a probe field is chirped around excitation frequency ν_0. Hence, hole burning provides a simple way to create a transparency window in an inhomogeneous medium. Once the hole is burnt, a signal pulse, whose spectrum is contained within the spectral hole, is sent through the crystal.

In order to investigate slow light, we aim at creating a TW as deep and narrow as possible. In our 0.5% Tm^{3+}:YAG-doped crystal, linear absorption coefficient is 5 cm^{-1}. Since both ground sublevels are equally populated before hole burning, one can increase the optical depth around ν_0 by pumping the ions around $\nu_0+\Delta_g$ and $\nu_0-\Delta_g$, thus building antiholes around ν_0. During the preparation step, one simultaneously pumps at the hole burning position ν_0 with AOM2 and over a few MHz-wide intervals centered at $\nu_0+\Delta_g$ and $\nu_0-\Delta_g$ with AOM1 [see Fig. 4(a)]. As already mentioned, our double-pass AOMs only manage a single frequency at a time. Therefore one has to chirp AOM1 alternatively around $\nu_0+\Delta_g$ and $\nu_0-\Delta_g$. Compound generation of both frequencies would give rise to spurious excitation around the beat note ν_0. With this procedure the available absorption is raised up to 8.5 cm^{-1}. The linear absorption coefficient around the spectral hole, with and without the absorption improvement sequence, is displayed in Fig. 4(b). In both cases, the hole is well described by a Lorentzian shape.

Once preparation is completed, we investigate the propagation of a weak signal, with a maximum power of ≈ 2 μW, through the spectral hole burnt at frequency ν_0. Figure 5 represents the transmission of 5.37-μs-long pulses through a spectral hole for various hole-width values. One varies the

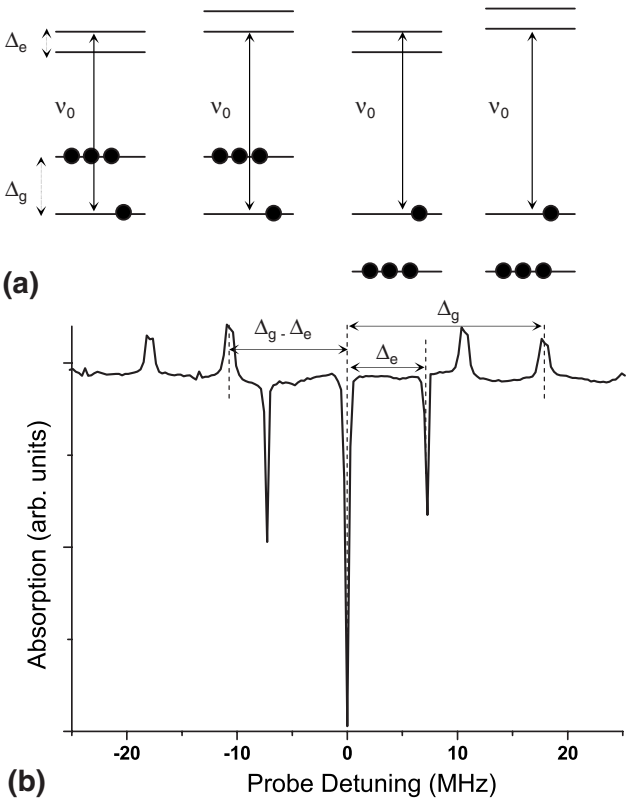

FIG. 3. Hole burning principle. (a) Simultaneous excitation of four classes of atoms by laser at frequency ν_0. Atoms, represented by circles, are pumped in the nonresonant ground sublevel. Δ_g and Δ_e, respectively, stand for ground and excited-state splittings. (b) Hole burning absorption spectrum. We have in this case $\Delta_g = 18$ MHz and $\Delta_e = 7.5$ MHz.

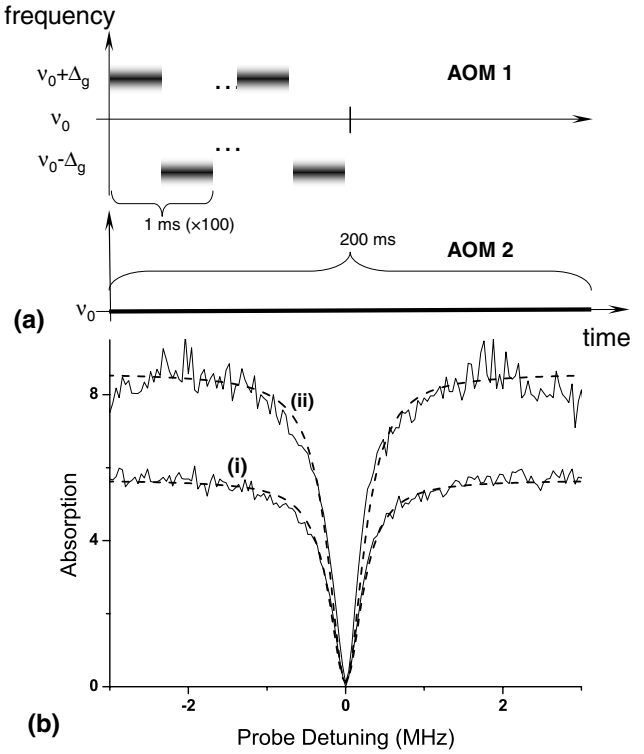

FIG. 4. (a) Time diagram of the hole burning sequence. Three different frequencies are involved in the preparation step. In addition to hole burning at ν_0, one increases the available optical depth by pumping around $\nu_0+\Delta_g$ and $\nu_0-\Delta_g$. AOM2 is used to burn the hole, while pumping to the hole region is accomplished by alternatively chirping AOM1 around $\nu_0+\Delta_g$ and $\nu_0-\Delta_g$. (b) Hole burnt at ν_0 with AOM1 (i) off and (ii) on. The maximum hole depth is 8.5 cm^{-1}.

hole width from 206 to 860 kHz by adjusting the pumping power from 10 to 300 μW. The origins of time and the input signal shape are given by a reference pulse that propagates through a 100% transmission, 10-MHz-wide spectral hole. For 860- and 420-kHz-wide holes, the pulse is not distorted and the delay is simply deduced from the maximum amplitude position. For the 200-kHz-wide hole, we measure a delay of 2 μs, which corresponds to a group velocity of 2500 ms^{-1}.

For a Lorentzian spectral hole, the delay experienced by a Gaussian pulse is simply expressed as $\alpha L/\Gamma$. In order to check this dependence, we measure the delay of the 5.37-μs-long Gaussian pulses as a function of the ratio $\alpha L/\Gamma$. To prevent pulse distortion, we keep the hole width larger than 600 kHz. We control $\alpha L/\Gamma$ by varying the hole depth. The measured delay is plotted as a function of the ratio $\alpha L/\Gamma$ in Fig. 6. The experimental data agree well with theoretical prediction.

IV. CONCLUSION

We have observed the slowing down of light produced by persistent spectral hole burning in a thulium-doped YAG crystal. The largest value of the observed delays, 2 μs, corresponds to a group-velocity reduction by a factor of more

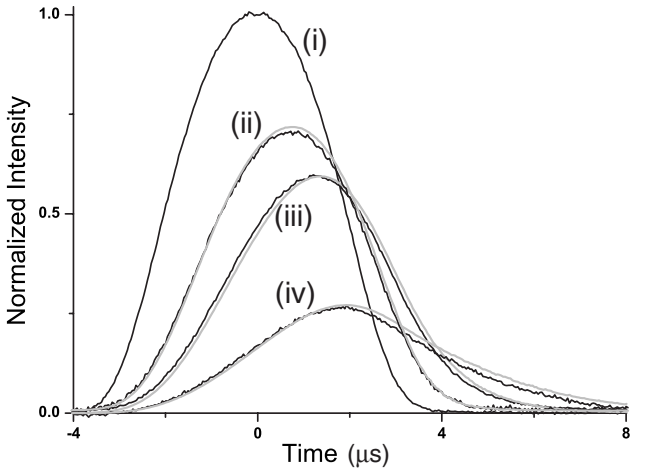

FIG. 5. Pulse propagation through several spectral holes. The input pulse coincides with the reference pulse (i). Transmission through holes of widths 860, 420, and 206 kHz, respectively, leads to the delayed, attenuated, and stretched profiles numbered from (ii) to (iv). The hole depth is maintained at 8.5 cm^{-1}. The theoretical profiles are completely determined by the hole width and depth. They are displayed as gray lines, together with the experimental data, represented by black lines.

than 10^5. A more concentrated and longer crystal may provide larger delays. Indeed, the fractional delay is limited by the opacity αL. The hole is burnt by optical pumping to another hyperfine sublevel. The long hyperfine state lifetime entails important consequences. On the one hand, taking advantage of the hole persistence, we were able to devise a sophisticated pumping scheme that enabled us to significantly increase the available opacity, which has resulted in an improved hole depth. On the other hand, the hole can be prepared long before the slow light observation, which eliminates the simultaneous presence of an intense control field. Analyzing the slowing down process, we have pointed out the role played by off-resonance atoms where most of the incoming information is carried over while the pulse is confined within the sample. This may open a way to quantum storage, quite in the same way as in EIT [20].

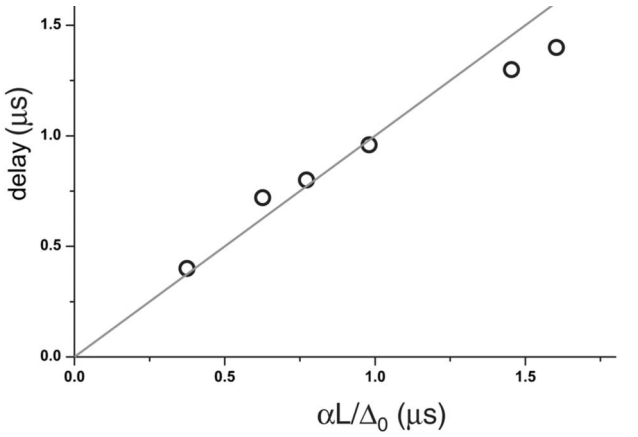

FIG. 6. Experimentally measured delays as a function of the measured ratio $\alpha L/\Gamma$. The delay caused by a Lorentzian hole is expected to equal this quantity.

[1] L. Brillouin, *Wave Propagation and Group Velocity* (Academic, New York, 1960).
[2] G. G. B. Garrett and D. E. McCumber, Phys. Rev. A **1**, 305 (1970).
[3] S. Chu and S. Wong, Phys. Rev. Lett. **48**, 738 (1982).
[4] L. J. Wang, A. Kuzmich, and A. Dogariu, Nature (London) **406**, 277 (2000).
[5] S. E. Harris, J. E. Field, and A. Imamoglu, Phys. Rev. Lett. **64**, 1107 (1990).
[6] R. M. Camacho, C. J. Broadbent, I. Ali-Khan, and J. C. Howell, Phys. Rev. Lett. **98**, 043902 (2007).
[7] M. D. Lukin, Rev. Mod. Phys. **75**, 457 (2003).
[8] S. E. Harris, Phys. Today **50**(7), 36 (1997).
[9] L. V. Hau, S. E. Harris, Z. Dutton, and C. H. Behroozi, Nature (London) **397**, 594 (1999).
[10] A. Kasapi, M. Jain, G. Y. Yin, and S. E. Harris, Phys. Rev. Lett. **74**, 2447 (1995).
[11] A. V. Turukhin, V. S. Sudarshanam, M. S. Shahriar, J. A. Musser, B. S. Ham, and P. R. Hemmer, Phys. Rev. Lett. **88**, 023602 (2001).
[12] J. J. Longdell, E. Fraval, M. J. Sellars, and N. B. Manson, Phys. Rev. Lett. **95**, 063601 (2005).
[13] C. Wei and N. B. Manson, Phys. Rev. A **60**, 2540 (1999).
[14] S. E. Schwarz and T. Y. Tan, Appl. Phys. Lett. **10**, 4 (1967).
[15] M. S. Bigelow, N. N. Lepeshkin, and R. W. Boyd, Phys. Rev. Lett. **90**, 113903 (2003).
[16] E. Baldit, K. Bencheikh, P. Monnier, J. A. Levenson, and V. Rouget, Phys. Rev. Lett. **95**, 143601 (2005).
[17] R. N. Shakhmuratov, A. Rebane, P. Mégret, and J. Odeurs, Phys. Rev. A **71**, 053811 (2005).
[18] A. Rebane, R. N. Shakhmuratov, P. Mégret, and J. Odeurs, J. Lumin. **127**, 22 (2007).
[19] R. M. Camacho, M. V. Pack, and J. C. Howell, Phys. Rev. A **74**, 033801 (2006).
[20] R. Lauro, T. Chanelière, and J.-L. Le Gouët, Phys. Rev. A **79**, 053801 (2009).
[21] F. Könz, Y. Sun, C. W. Thiel, R. L. Cone, R. W. Equall, R. L. Hutcheson, and R. M. Macfarlane, Phys. Rev. B **68**, 085109 (2003).
[22] D. Grischkowsky, Phys. Rev. A **7**, 2096 (1973).
[23] E. Courtens, Phys. Rev. Lett. **21**, 3 (1968).
[24] S. L. McCall and E. L. Hahn, Phys. Rev. Lett. **18**, 908 (1967).
[25] F. de Seze, A. Louchet, V. Crozatier, I. Lorgeré, F. Bretenaker, J.-L. Le Gouët, O. Guillot-Noël, and Ph. Goldner, Phys. Rev. B **73**, 085112 (2006).
[26] V. Crozatier, F. de Sèze, L. Haals, F. Bretenaker, I. Lorgeré, and J.-L. Le Gouët, Opt. Commun. **241**, 203 (2004).
[27] A. Louchet, J. S. Habib, V. Crozatier, I. Lorgeré, F. Goldfarb, F. Bretenaker, J.-L. Le Gouët, O. Guillot-Noël, and Ph. Goldner, Phys. Rev. B **75**, 035131 (2007).